Translational Research in Anatomy 33 (2023) 100263

Contents lists available at ScienceDirect

Translational Research in Anatomy

journal homepage: www.elsevier.com/locate/tria

Quantitative characterization of age-related atrophic changes in cerebral hemispheres: A novel "contour smoothing" fractal analysis method

Nataliia Maryenko *, Oleksandr Stepanenko

Department of Histology, Cytology and Embryology, Kharkiv National Medical University, Kharkiv, Ukraine

ARTICLE INFO

Keywords:
Aging
Cerebral hemispheres
Fractal analysis
Morphometry
MRI
Neuroimaging

ABSTRACT

Background: Quantitatively assessing age-related atrophic changes in cerebral hemispheres remains a crucial challenge, particularly in distinguishing between normal and pathological brain atrophy caused by neurodegenerative diseases. In this study, we introduced a new fractal analysis algorithm, referred to as the "contour smoothing" method, to quantitatively characterize age-related atrophic changes in cerebral hemispheres.

Materials and methods: MRI scans from 100 healthy individuals (44 males, 56 females), aged 18–86 (mean age 41.72 ± 1.58), were analyzed. We used two fractal analysis methods: the novel "contour smoothing" method (with stages: 1–6, 1–5, 2–6, 1–4, 2–5) and the classical "box-counting" method to assess cerebral cortex pial surface contours.

Results: Fractal dimensions obtained using the "box-counting" method showed weak or statistically insignificant correlations with age. Conversely, fractal dimensions derived from the "contour smoothing" method exhibited significant age-related correlations. The "contour smoothing" method with 1–4 stages proved more suitable for quantifying atrophic changes. The average fractal dimension for 1–4 coronal sections was 1.402 ± 0.005 (minimum 1.266, maximum 1.490), and for all five tomographic sections, it was 1.415 ± 0.004 (minimum 1.278, maximum 1.514). These fractal dimensions exhibited the strongest correlations with age: $r = -0.709$ ($p < 0.001$) and $r = -0.669$ ($p < 0.001$), respectively.

Conclusion: The "contour smoothing" fractal analysis method introduced in this study can effectively examine cerebral hemispheres to detect and quantify age-related atrophic changes associated with normal or pathological aging. This method holds promise for clinical application in diagnosing neurodegenerative disorders, such as Alzheimer's disease.

1. Introduction

In the cerebral hemispheres, significant changes in their spatial configuration can occur throughout life as a result of age-related atrophy. These changes encompass the smoothing of the cerebral surface, widening and deepening of sulci, reduction in size, and simplification of gyral shape. Such alterations typically result from the normal brain aging process [1–6]. However, a substantial group of neurodegenerative disorders, including Alzheimer's disease, also leads to atrophic changes resembling those observed in normal aging [7–9]. Atrophic changes in the cerebral hemispheres can be detected in vivo through diagnostic neurovisualization methods, such as structural magnetic resonance imaging (MRI) [7–9]. Physicians performing brain tomogram evaluations must address critical questions: Does this patient exhibit atrophic changes in cerebral hemispheres? How pronounced are the identified atrophic changes? Are the observed cerebral atrophic changes a consequence of normal brain aging, or do they indicate the presence of a neurodegenerative disorder?

In recent decades, researchers aiming to quantitatively characterize cerebral atrophic changes and features of cerebral structure have utilized the following parameters: volumes of gray and white matter [1–6], cortical thickness [4–6], gyrification index [4,6], sulcal depth [4,6], and folding area [6]. The determination of these morphometric parameters is based on methods from Euclidean geometry. Additionally, fractal analysis – the method of fractal geometry – can be employed for morphometry [10,11]. Fractal analysis quantifies the fractal dimension (FD), a measure of the space-filling capacity of a particular structure, serving as an indicator of its complexity [10,11]. As atrophic changes lead to a simplification of brain shape (resulting in reduced spatial configuration complexity), the FD can serve not only as a quantitative

* Corresponding author. Department of Histology, Cytology and Embryology, Kharkiv National Medical University, Kharkiv, 4 Nauky avenue, 61022, Ukraine.
E-mail addresses: maryenko.n@gmail.com, ni.marienko@knmu.edu.ua (N. Maryenko), oy.stepanenko@knmu.edu.ua (O. Stepanenko).

https://doi.org/10.1016/j.tria.2023.100263
Received 16 August 2023; Received in revised form 8 September 2023; Accepted 11 September 2023
Available online 13 September 2023

measure of shape complexity but also as a tool to determine the presence of cerebral atrophic changes and quantitatively characterize them. Fractal analysis has been employed in several studies for the morphometry of MRI brain images [5,12–22], including the characterization of brain changes in normal aging [5,12–14,22], Alzheimer's disease [15,16], and multiple sclerosis [17–19].

However, fractal analysis is not yet widely used in clinical practice. One of the factors hindering the clinical application of fractal analysis is the relative complexity of the algorithms used for preprocessing MRI images and determining the FD. In the majority of cerebral MRI image studies, the three-dimensional (3D) version of fractal analysis has been utilized [5,6,12–14,16–19]. This approach holds undeniable advantages, as it comprehensively assesses the shape of cerebral hemispheres: the FD captures the spatial complexity of the entire studied structure – cortical ribbon, cortical surface, white matter, or brain tissue as a whole. The 3D variants of fractal analysis involve constructing 3D brain models, subsequently analyzed using specialized software. However, constructing 3D brain models is complex and often impractical for routine clinical use, particularly in developing countries due to factors like poor MRI image quality, excessive thickness of tomographic sections, lack of available software, and limited opportunities for neuro-radiologists to undergo 3D modeling training. Studying two-dimensional (2D) tomographic sections is a routine daily practice [22]; therefore, the development of effective 2D modifications of fractal analysis with user-friendly and implementable algorithms remains a pertinent scientific endeavor.

In this study, our objective was to develop simple, user-friendly and clinically applicable algorithm for fractal analysis of 2D MRI brain images, aiming to detect and quantitatively characterize age-related atrophic changes in the cerebral hemispheres. We chose to investigate the spatial configuration of the cortical pial surface of the cerebral hemispheres, as it exhibits fractal properties [23], and atrophic brain changes primarily manifest in alterations of its visible surface configuration. For the development of the fractal analysis algorithm, we based our approach on Richardson's method (Caliper, Perimeter stepping) [24,25]. Its classical version is non-automated and therefore complicated for use in morphometric studies. In our previous work, we described our own modification of Richardson's method [26]. In this study, we further developed and adapted this methodology for the quantitative characterization of age-related atrophic changes in the cerebral hemispheres. Due to the methodology's features, we decided to name this modification the "contour smoothing" method. Additionally, we employed the "box-counting" method in its 2D variant, which currently serves as the "gold standard" among fractal analysis methods in medicine and morphology due to its relative simplicity and universality [25]. This allowed us to compare results obtained using both fractal analysis methods.

2. Material and methods

2.1. Participants of the study

This study involved the analysis of MRI brain scans from 100 apparently healthy individuals, ranging in age from 18 to 86 years (mean age 41.72 ± 1.58 years). The study participants underwent diagnostic MRI brain scanning and showed no apparent brain pathology upon examination, and their MRI data were considered as relatively normal. The sample encompassed 44 males (mean age 41.43 ± 1.68 years) and 56 females (mean age 41.95 ± 1.51 years). Thirty-one individuals were aged 18–30 years (14 males and 17 females), 29 individuals were aged 31–45 years (14 males and 15 females), 24 individuals were aged 46–60 years (8 males and 16 females), and 16 individuals were aged 61–86 years (8 males and 8 females).

2.2. MRI protocol

The MRI images were acquired using a Siemens Magnetom Symphony magnetic resonance scanner with a magnetic induction of 1.5 T. The T2 and FLAIR modes were employed with the following parameters: T2 mode – echo time (TE) of 130 ms, repetition time (TR) of 4440 ms, and a section thickness of 5 mm; FLAIR mode – TE of 114 ms, TR of 9000 ms, inversion time (TI) of 2500 ms, and a section thickness of 5 mm. The digital MRI images had a spatial resolution of 72 pixels per inch, and the absolute image scale was 3 pixels = 1 mm.

2.3. Selection of MRI images

For the investigation of each brain, five tomographic sections were selected, including four sections in the coronal (frontal) projection and one section in the axial (horizontal) projection (Fig. 1). We chose tomographic sections easily identifiable by anatomical landmarks and corresponding to different regions of the cerebral hemispheres. These sections correspond to areas of the brain where pathological changes are most commonly detected in certain neurodegenerative diseases, including Alzheimer's disease [15]. The first coronal tomographic section was positioned at the level of the most anterior points of the temporal lobes, the second at the level of the mammillary bodies (*corpus mamillare*), the third at the level of the quadrigeminal plate (*lamina quadrigemina*), and the fourth at the level of the splenium of the corpus callosum (*splenium corpori callosi*). The axial section was defined as the most superficially located tomographic section containing thalamic structures; thus, considering a section thickness of 5 mm, this section corresponded to the upper part of the thalamus.

2.4. Fractal analysis: a novel "contour smoothing" method

To develop the "contour smoothing" fractal analysis method, we utilized Adobe Photoshop CS5 software. Initially, we selected an area of the MRI image corresponding to the tissue of the cerebral hemispheres: we delineated it specifically following the pial surface of the cortex (Fig. 2, A, Video supplement). The "selection" tool was used for that purpose. Additional image processing, such as segmentation or the contour outlining, was not required (the contour of the selected area in Fig. 2 was outlined with a blue line for illustrative clarity).

Various fractal analysis algorithms typically involve multiple stages (iterations). For the developed "contour smoothing" method, we employed six stages (Fig. 2, A-F, Table 1). At the first stage, the perimeter (P) of the selected area was measured using the "analysis" tool, and no contour modification was performed (Fig. 2, A). Starting from the second stage, we modified the contour using the "smoothing" tool. This tool removes distorted sections (protrusions, invaginations) from the contour that have a curvature radius smaller than the specified smoothing radius (R). The R value was set to 2 pixels (2/3 mm) at the second stage, 4 pixels (4/3 mm) at the third stage, 8 pixels (8/3 mm) at the fourth stage, 16 pixels (16/3 mm) at the fifth stage, and 32 pixels (32/3 mm) at the sixth stage (Fig. 2, B–F, Video supplement). Thus, contour sections corresponding to sulci were gradually removed in each stage of the fractal analysis, with narrower sulci removed in the earlier stages and wider sulci in the subsequent ones. As a result of this step-by-step modification, the contour became nearly completely smooth by the final stage of fractal analysis (Fig. 2, F). Similar to the first stage, the P value was measured after each contour modification during the second to sixth stages.

For calculating the FD value, we used the P and R values determined at each of the six stages of fractal analysis (Table 1). Natural logarithms of two values were calculated: the reciprocal of the smoothing radius (1/R), and the perimeter divided by the smoothing radius (P/R). Considering that smoothing was not applied at the first stage of fractal analysis, the value of R for the first stage was considered equal to one.

Based on the obtained values, a linear regression equation $y=b\times x+a$

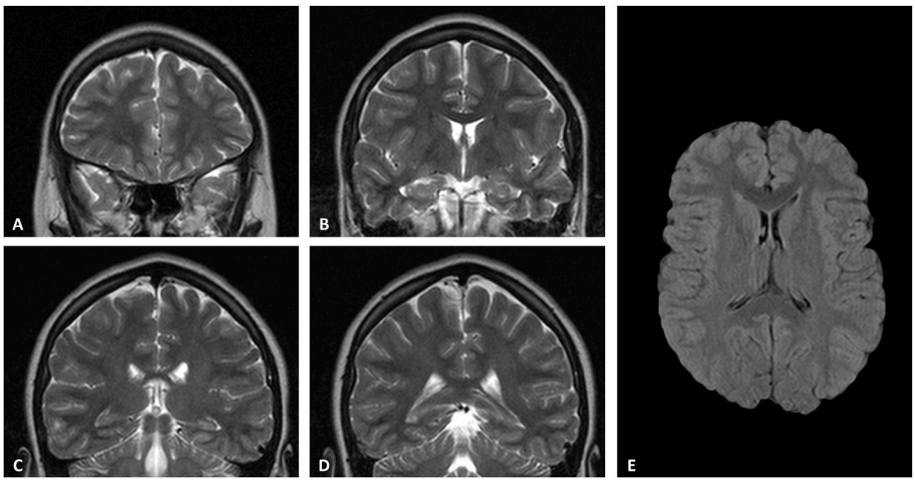

Fig. 1. MRI brain images selected for the study (18 years old female individual). A – 1st coronal section (level of the anterior pole of the temporal lobes), B – 2nd coronal section (level of the mammillary bodies), C – 3rd coronal section (level of the quadrigeminal plate), D – 4th coronal section (level of the splenium of the corpus callosum), E – axial section (level of the thalamus). A-D – T2-weighted mode, E – FLAIR mode.

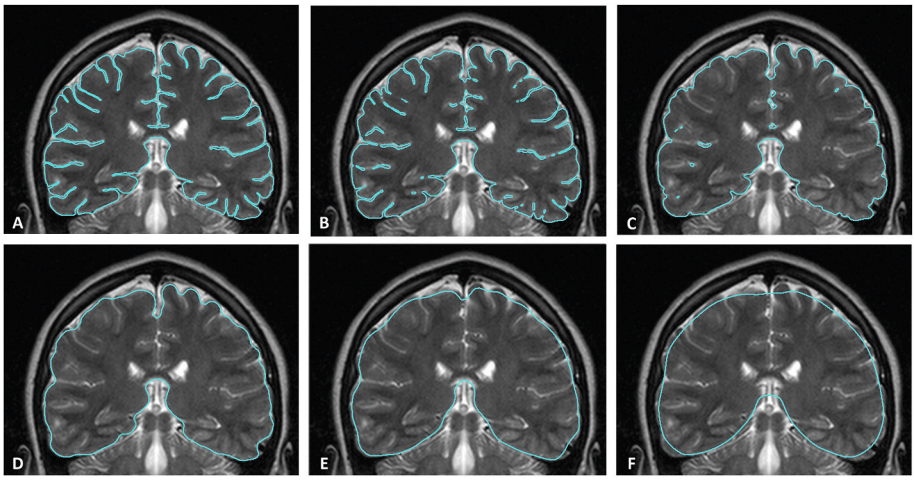

Fig. 2. Fractal analysis, "contour smoothing" method. The outer contour of the cerebral hemispheres (following the pial surface of the cortex) was outlined with a blue line for illustrative clarity. Stages of fractal analysis: A – 1st stage, contour without smoothing; B – 2nd stage, smoothing with a radius of 2 pixels; C – 3rd stage, smoothing with a radius of 4 pixels; D – 4th stage, smoothing with a radius of 8 pixels; E – 5th stage, smoothing with a radius of 16 pixels; F – 6th stage, smoothing with a radius of 32 pixels.

Table 1
Data for calculating FD using the contour smoothing method.

Stage of Fractal analysis	Parameter					
	R Smoothing radius	1/R	P Perimeter	P/R	LN(1/R)	LN (P/R)
1	1[a]	1	4445	4445	0.000	8.400
2	2	0.5	2545	1272.5	−0.693	7.149
3	4	0.25	1749	437.25	−1.386	6.081
4	8	0.125	1560	195	−2.079	5.273
5	16	0.0625	1386	86.625	−2.773	4.462
6	32	0.03125	1284	40.125	−3.466	3.692

[a] The R value for the first stage was considered equal to one for the FD calculations.

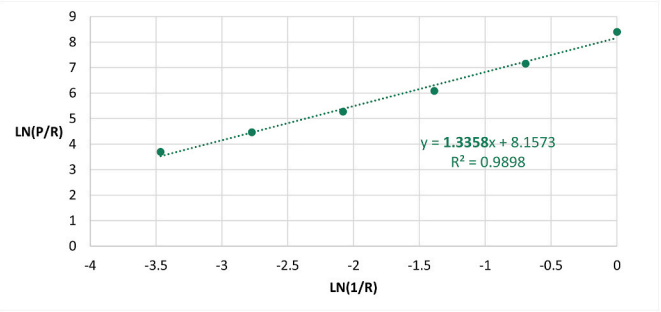

Fig. 3. Fractal analysis, "contour smoothing" method. Calculation of linear regression equation and determination of FD. In this example, the FD is equal to 1.3358.

was calculated, where the independent variable *x* represented the value of LN(1/R), and the dependent variable *y* represented the value of LN(P/R); the FD corresponded to the coefficient *b*, which was the estimated slope of the regression line, and the coefficient *a* was the estimated intercept (Fig. 3). Thus, the FD based on the example calculations (Fig. 2, Table 1) was 1.3358 (Fig. 3).

Fractal analysis may involve varying numbers of stages, depending on the methodology and the object under investigation. Since this study involved the development of a new algorithm, we attempted to calculate FD values based not only on data from all six stages of fractal analysis but also on a limited number of stages. Thus, for each of the 500 tomographic sections selected for the study, five FD values were calculated, including one based on all stages of fractal analysis (1–6) and four based on a reduced number of stages (1–5, 2–6, 1–4, 2–5). The summarized "contour smoothing" algorithm (for stages 1–4) is illustrated in

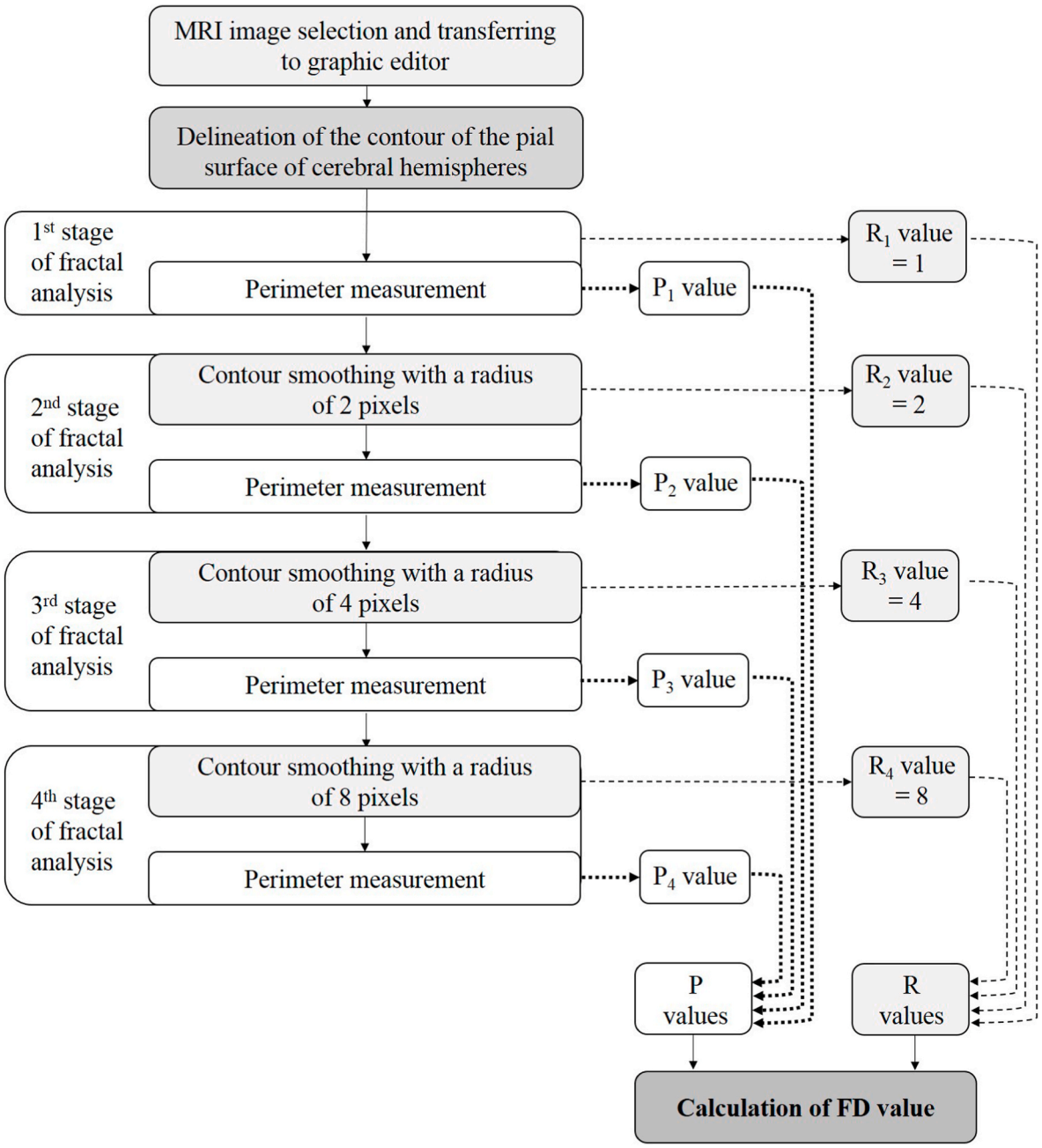

Fig. 4. Fractal analysis, "contour smoothing" algorithm (1–4 stages).

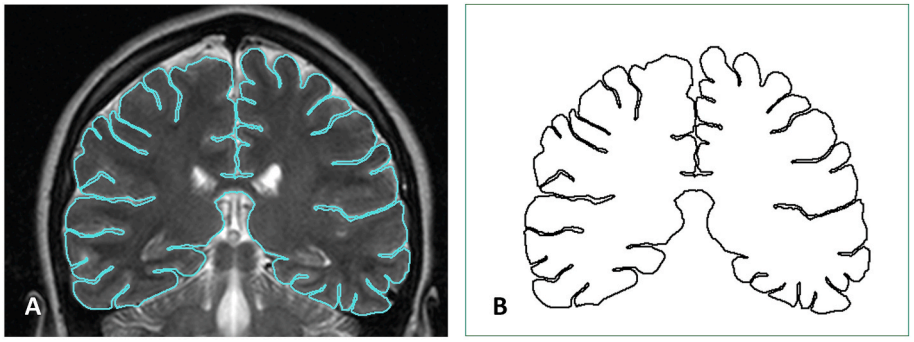

Fig. 5. Image preprocessing for the "box-counting" fractal analysis method: A – selection of the cerebral hemispheres area, B – outlining of the pial cortical surface contour.

Fig. 4 (see also video supplement).

2.5. Fractal analysis: existing "box-counting" method

For fractal analysis provided by "box-counting" method, we utilized the "fractal box count" tool of the Image J software [27]. This image analysis tool necessitates preliminary image processing. After selecting the cerebral hemispheres area (Fig. 5, A), we outlined the contour of the pial cortical surface using a black line, 1 pixel in thickness, and filled the background with white color. (Fig. 5, B). As a result, a binary image was generated, consisting of white and black pixels. This supplementary image preprocessing step was applied specifically for the "box-counting" method and was not employed for the "contour smoothing" method.

2.6. Euclidean geometry-based morphometry

In addition to FD values, the morphometric parameters belonging to Euclidean geometry were determined: perimeter (P), area (A), and derived indices based on them. To determine the P and A values, we utilized the "selection" and "analysis" tools of Adobe Photoshop CS5 software: the cerebral hemispheres area was outlined on the image, and then its P and A values were calculated in two variants (Fig. 6A and B). Initially, the tomographic sections were outlined according to their external (visible) surface, disregarding the sulci (Fig. 6, A); the P_A value, determined in this variant, corresponded to the contour length of the visible surface of the cerebral hemispheres, and the A_A value represented the overall brain tissue area, including the sulci content. Subsequently, the entire pial surface was outlined on the tomographic sections, considering the sulci (Fig. 6, B); the P_B value of which corresponded to the contour length of the pial surface of the cerebral hemispheres (including the contour inside sulci), and the A_B value represented the overall brain tissue area (excluding the sulci content). The following derived indices were also computed: perimeter-to-area ratios (P_A/A_A and P_B/A_B), shape factors (SF_A and SF_B), perimeter ratios (P_B/P_A), and area ratios (A_B/A_A). To calculate the SF value, we used the formula: $SF=(4\pi \times A)/P^2$ [28]. The ratio of the two perimeters (P_B/P_A) can be considered as a 2D analogue of the gyrification index, as this index characterizes the ratio of the total contour length of the cerebral hemispheres' surface to the length of the contour of their superficially exposed surface.

2.7. Statistics

Statistical data analysis was conducted using Microsoft Excel 2016 software. The data were processed using tools of variation statistics. For each FD variation series, the following statistical parameters were calculated: arithmetic mean (M), its standard error (m), minimum (Min), and maximum (Max) values. The significance of statistical differences between FD values of tomographic sections with different localizations was assessed using the Kruskal–Wallis H test and post-hoc Dunn's test with Bonferroni adjustment for multiple comparisons. The significance of statistical differences between FD values in men and women (pairwise comparisons) was assessed using Student T test. To compare the linear regression equations Fisher's F test was applied. To assess the interrelationships of the obtained values, the Pearson correlation coefficient (r) was calculated, and its significance was evaluated using the Student T test. The significance level for all results was accepted as $p < 0.05$.

3. Results

3.1. FD values

The FD values, computed using two fractal analysis methods, are given in Table 2.

For multiple comparisons of FD values determined using different stages of the "contour smoothing" method and the "box-counting" method, the Kruskal-Wallis test was employed. Initial assessment indicated significant differences in FD values ($p \approx 0$ for all localizations). Subsequently, the Dunn's test was utilized to identify which specific FD values differed significantly. It was found that FD values determined using the "box-counting" method significantly differed from all FD values obtained via the "contour smoothing" method across all possible variations and localizations ($p < 0.05$) except for the axial section ($p > 0.05$). While most FD values determined using various stages of the fractal analysis also significantly differed from each other, a subset of FD values did not exhibit statistically significant differences. These included the FD values derived from stages 1–5 and 2–5 (1st to 4th coronal sections, average FD value of five tomographic sections and average FD value of 1–4 coronal sections), FD values obtained from stages 1–5 and 1–4 (1st and 2nd coronal sections, average FD value of 1–4 coronal sections), FD values from stages 1–6 and 2–6 (1st to 4th coronal sections), FD values from stages 1–4 and 2–5 (1st and 2nd coronal sections), and FD values from stages 1–6 and 2–5 (axial section).

3.2. Correlation of FD with age and fitting of fractal analysis algorythm

To determine the most suitable method and range of stages of fractal analysis that characterize age-related atrophic changes in the cerebral hemispheres, we assessed the correlation between FD values and age (Table 3).

It was found that the FD values obtained through the classic "box-counting" method did not exhibit statistically significant correlations with age, or these correlations were weak. Some of the FD values derived from the new "contour smoothing" method exhibited statistically significant correlations with age. Specifically, the strongest correlations with age were observed for FD values obtained using the 1–4 stages of fractal analysis, whereas the 1–6 stages of fractal analysis and other

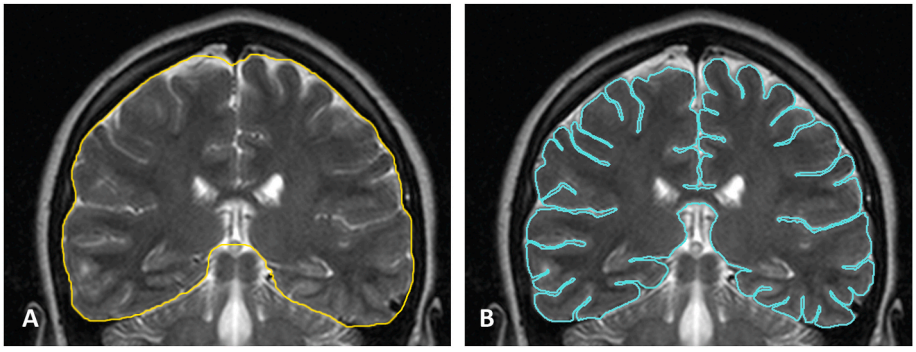

Fig. 6. Determination of morphometric parameters using Euclidean geometry methods: two variants of perimeter and area defining on the tomographic sections of the cerebral hemispheres.

Table 2
FD values of linear contour of the cerebral hemispheres.

Tomographic section	Parameter	Fractal analysis method					
		"Contour smoothing" method					"Box-counting" method
		Stages of fractal analysis					
		1–6	1–5	2–6	1–4	2–5	
1st coronal	M	**1.346**	**1.386**	**1.337**	**1.398**	**1.398**	**1.286**
	m	0.004	0.004	0.007	0.006	0.008	0.003
	Min	1.256	1.310	1.147	1.243	1.180	1.233
	Max	1.445	1.509	1.507	1.550	1.575	1.356
2nd coronal	M	**1.337**	**1.377**	**1.325**	**1.394**	**1.384**	**1.252**
	m	0.003	0.004	0.006	0.007	0.007	0.003
	Min	1.266	1.227	1.183	1.178	1.221	1.188
	Max	1.424	1.458	1.460	1.496	1.538	1.318
3rd coronal	M	**1.324**	**1.372**	**1.292**	**1.410**	**1.350**	**1.243**
	m	0.003	0.003	0.007	0.005	0.008	0.002
	Min	1.246	1.287	1.131	1.246	1.157	1.197
	Max	1.406	1.470	1.423	1.511	1.540	1.296
4th coronal	M	**1.322**	**1.370**	**1.289**	**1.408**	**1.348**	**1.243**
	m	0.003	0.003	0.006	0.005	0.007	0.002
	Min	1.243	1.298	1.151	1.275	1.192	1.189
	Max	1.385	1.440	1.415	1.524	1.497	1.304
Axial	M	**1.319**	**1.387**	**1.254**	**1.466**	**1.324**	**1.233**
	m	0.005	0.005	0.009	0.006	0.011	0.003
	Min	1.231	1.294	1.108	1.287	1.138	1.153
	Max	1.477	1.524	1.543	1.613	1.637	1.292
Average value (all sections)	M	**1.330**	**1.378**	**1.299**	**1.415**	**1.361**	**1.251**
	m	0.003	0.003	0.006	0.004	0.006	0.002
	Min	1.270	1.303	1.167	1.278	1.205	1.217
	Max	1.398	1.455	1.429	1.514	1.503	1.288
Average value (1–4 coronal sections)	M	**1.332**	**1.376**	**1.311**	**1.402**	**1.370**	**1.256**
	m	0.003	0.003	0.006	0.005	0.006	0.002
	Min	1.271	1.299	1.166	1.266	1.199	1.218
	Max	1.391	1.448	1.414	1.490	1.494	1.293

Table 3
Correlation coefficients (r) characterizing relationships between FD values of linear contour of the cerebral hemispheres and age.

Tomographic section	Fractal analysis method					
	"Contour smoothing" method					"Box-counting" method
	Stages of fractal analysis					
	1–6	1–5	2–6	1–4	2–5	
1st coronal	−0.024	−0.364***	0.255*	**−0.566*****	0.081	−0.070
2nd coronal	0.056	−0.293**	0.403***	**−0.511*****	0.240*	−0.220*
3rd coronal	0.297**	−0.070	0.543***	**−0.634*****	0.445***	−0.144
4th coronal	0.220*	−0.128	0.480***	**−0.554*****	0.391***	−0.285**
Axial	0.255*	0.131	0.368***	−0.182	0.348***	0.137
Average value (all sections)	0.224*	−0.201*	0.494***	**−0.669*****	0.392***	−0.171
Average value (1–4 coronal sections)	0.166	−0.305**	0.484***	**−0.709*****	0.352***	−0.250*

Note: * – $p < 0.05$; ** – $p < 0.01$; *** – $p < 0.001$, Student T test.

ranges of stages appeared less sensitive to age-related changes.

To investigate the impact of the selected range of fractal analysis stages on FD values, we selected two subjects – two tomographic sections (3rd coronal) of a young individual (18 years old) with no visually apparent atrophic changes in the brain (Fig. 7, A), and an elderly individual (76 years old) with visually apparent atrophic changes in the brain – sulcal widening and deepening, flattening of gyri (Fig. 7, B). However, this preliminary assessment was subjective and descriptive. During contour smoothing, we observed that in the young individual with no atrophic changes, the smoothing of sulci occurred in the initial stages of fractal analysis, as they were narrower compared to the elderly individual. Therefore, by the 4th stage, a nearly smooth contour (without sulci) was obtained. Since atrophic changes (in the elderly) lead to sulcal widening, their contours were less smoothed in the early stages of fractal analysis and persisted until the 4th stage, but were smoothed by the 6th stage. By employing the 1–6 stages of fractal analysis, in both cases (young and elderly individuals), we have a "long" contour initially (with sulci) and a smoothed, "short" contour at the 6th stage. However, by using the 1–4 stages of fractal analysis, in both cases, we have a "long" contour initially and a smoothed, "short" contour at the 4th stage in young individual, and a partially smoothed "long" contour in the elderly (Fig. 7).

Based on the data from the fractal analysis of the tomographic sections shown in Fig. 7, we calculated the linear regression equations using the 1–6 and 1–4 stages of fractal analysis (Fig. 8A and B).

Using the 1–6 stages of fractal analysis, we obtained the following FD values: 1.3358 (18 years old) and 1.3576 (76 years old) – these FD values were close, with the FD values of the elderly individual slightly exceeding those of the young individual. When we limited the number of fractal analysis stages to four, we obtained the following FD values: 1.5073 (18 years old) and 1.2937 (76 years old). These FD values differed – the FD of the brain's linear contour in the young individual significantly exceeded that of the elderly individual.

Thus, for conducting fractal analysis aimed at quantitatively

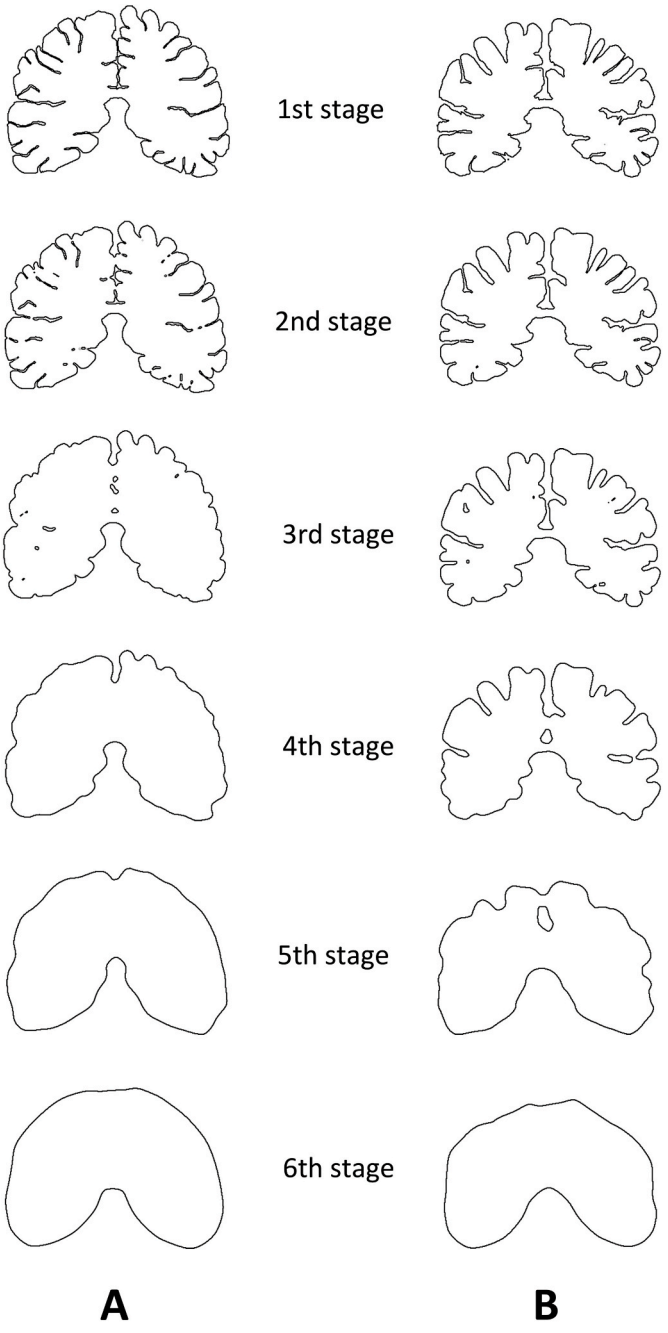

Fig. 7. Fractal analysis, "contour smoothing" method. 3rd coronal section. The outer contour of the cerebral hemispheres was outlined with a black line for illustrative clarity. A – 18-year-old female individual, B – 76-year-old male individual.

characterizing atrophic changes, the "contour smoothing" method using the 1–4 stages proved to be more suitable. Therefore, in further calculations, we used the FD values computed using this algorithm.

The sample size used in this study (N = 100) was sufficient for obtaining reliable results, allowing us to calculate confidence intervals for the FD values. These intervals can be used as norm criteria for performing brain MRI assessment in clinical practice (Fig. 9).

The strongest correlation with age was observed in the FD values of the 1–4 coronal sections and their mean value. In contrast, the FD values of axial sections showed no significant correlation with age. This can be explained by anatomical differences: in the coronal (frontal) projection, most sulci and gyri are cut perpendicularly or at angles close to a right angle. As a result, in the outlined contour of pial surface of the cortex,

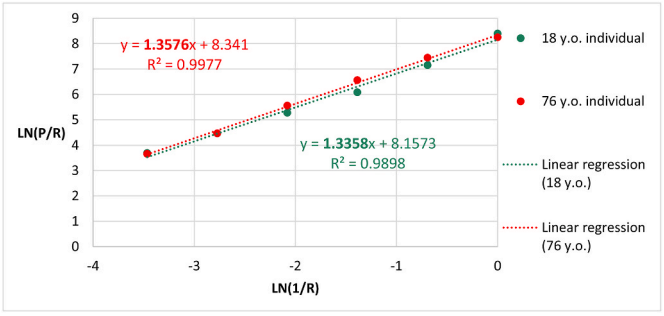

Fig. 8 A. Fractal analysis, "contour smoothing" method. Calculation of FD in young and elderly individuals based on the 1–6 stages of fractal analysis: insignificant difference in FD values.

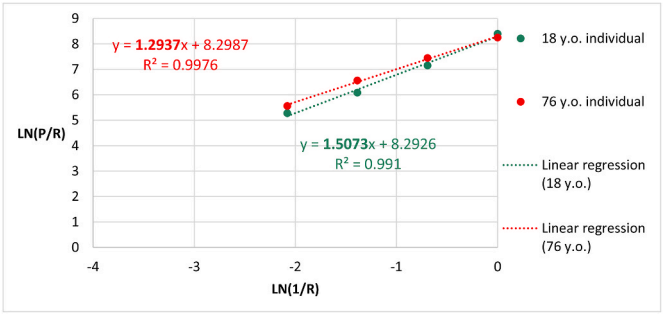

Fig. 8 B. Fractal analysis, "contour smoothing" method. Calculation of FD in young and elderly individuals based on the 1–4 stages of fractal analysis: significant difference in FD values.

sulci appear as invaginations branching off at an angle close to a right angle, which is favorable for accurate smoothing. In axial sections, the orientation of sulci and gyri is slightly different, and the angles at which the contour of the sulci deviates from the outer contour are multiform. Therefore, the most informative results using our proposed fractal analysis method are obtained from the study of coronal tomographic sections.

An additional observation is that the strongest correlation with age was noted in the average FD value of the 1–4 coronal sections ($r = -0.709$), surpassing the correlation strength of each individual coronal section. This can be attributed to an overall cumulative effect: when computing the mean FD value, alterations in multiple brain regions are simultaneously considered, potentially mitigating the influence of value dispersion. It is reasonable to posit that employing a larger number of coronal sections for analysis could enhance the correlation strength between the average FD value and age.

When comparing the FD values determined from five tomographic sections using 1–4 stages of fractal analysis, it was found that the FD values significantly differed from each other ($p \approx 0$, assessed using the Kruskal-Wallis H test with Bonferroni adjustment for multiple comparisons). Further pairwise comparisons of different tomographic sections through the Dunn test revealed that the FD values of the 1st, 2nd, 3rd, and 4th coronal sections did not significantly differ from each other ($p > 0.05$); however, they significantly differed from the FD value of the axial section ($p < 0.001$ for all pairwise comparisons between the FD of the axial section and FD of the 1st, 2nd, 3rd, and 4th coronal sections).

3.3. FD values in men and women

The FD values in men and women across all investigated regions of the cerebral hemispheres did not show statistically significant differences ($p > 0.05$ for all examined tomographic sections, Student T test) (Table 4).

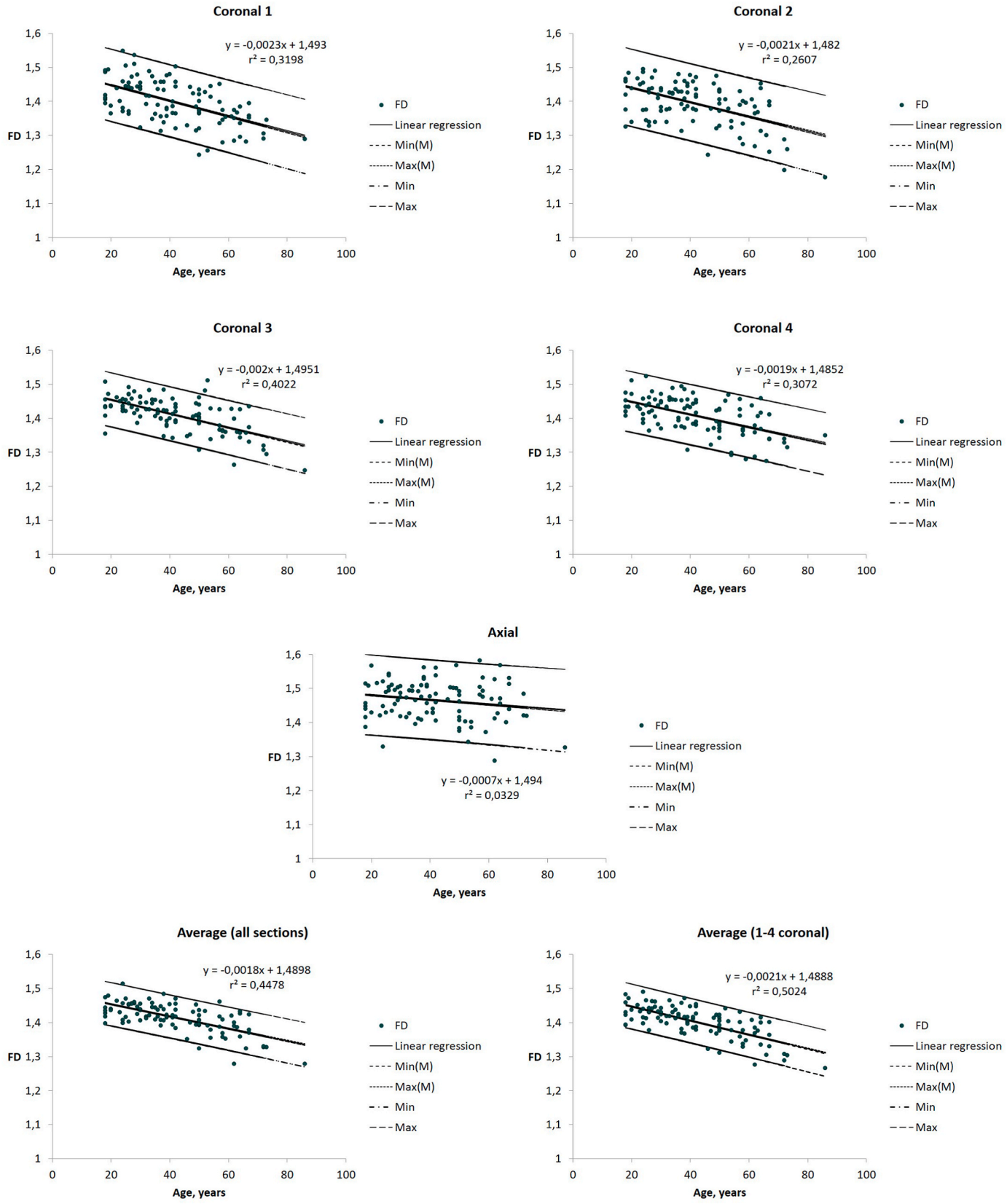

Fig. 9. Age dynamics and confidence intervals of the FD values of cerebral hemispheres contour, computed using the "contour smoothing" method, employing 1–4 stages of fractal analysis.

Table 4
FD values of cerebral hemispheres contour obtained using "contour smoothing" method (stages 1–4) in men and women.

Tomographic section	Parameter	Sex group	
		Male	Female
Coronal 1	**M**	**1.388**	**1.405**
	m	0.010	0.008
	Min	1.243	1.28
	Max	1.55	1.537
Coronal 2	**M**	**1.386**	**1.400**
	m	0.011	0.008
	Min	1.178	1.199
	Max	1.496	1.491
Coronal 3	**M**	**1.403**	**1.415**
	m	0.009	0.006
	Min	1.246	1.307
	Max	1.511	1.504
Coronal 4	**M**	**1.401**	**1.413**
	m	0.009	0.006
	Min	1.275	1.291
	Max	1.511	1.524
Axial	**M**	**1.463**	**1.468**
	m	0.01	0.007
	Min	1.287	1.329
	Max	1.613	1.568
Average (all sections)	**M**	**1.408**	**1.420**
	m	0.007	0.005
	Min	1.278	1.327
	Max	1.514	1.478
Average(1–4 coronal)	**M**	**1.394**	**1.408**
	m	0.008	0.006
	Min	1.266	1.288
	Max	1.49	1.483

The FD values in both men and women exhibited a tendency to decrease with age, similar to the case of the entire sample analyzed (Fig. 10). During the correlation analysis, we obtained the following correlation coefficient values between FD values and age: 1st coronal section: men $r = -0.504$, $p < 0.001$, women $r = -0.640$, $p < 0.001$; 2nd coronal section: men $r = -0.583$, $p < 0.001$, women $r = -0.450$, $p < 0.001$; 3rd coronal section: men $r = -0.578$, $p < 0.001$, women $r = -0.719$, $p < 0.001$; 4th coronal section: men $r = -0.595$, $p < 0.001$, women $r = -0.524$, $p < 0.001$; axial section: men $r = -0.400$, $p < 0.01$, women $r = 0.058$, $p > 0.05$; average FD value of all sections: men $r = -0.697$, $p < 0.001$, women $r = -0.665$, $p < 0.001$; average FD value of 1–4 coronal sections: men $r = -0.712$, $p < 0.001$, women $r = -0.729$, $p < 0.001$.

We also compared the linear regression equations characterizing the relationships between FD (dependent variable) and age (independent variable) (Fig. 10); no statistically significant differences in age-related dynamics between men and women were found ($p \approx 1$ for all examined tomographic sections, Fisher's F test). Given the lack of substantial differences between gender groups, we did not divide the sample into groups based on sex for further analysis.

3.4. Correlation analysis: FD values and euclidean geometry

During the correlation analysis, it was observed that the strongest correlations existed between the FD values of adjacent coronal sections: 1 and 2, 2 and 3, 3 and 4 (Table 5). This phenomenon could be attributed to regional anatomical features that influenced the shape characteristics of the brain within adjacent regions.

Among the morphometric parameters determined using Euclidean geometry methods, the P_B value and the P_B/P_A value exhibited the strongest correlations with FD. These parameters indirectly characterize the curvature of the linear contour. Additionally, the A_B/A_A value also displayed significant correlation with FD (Table 6).

4. Discussion

Fractal analysis has been employed in a number of studies to characterize atrophic changes in the cerebral hemispheres during both normal and pathological aging [5,12–16,20–22]. Among the most comprehensive investigations into the age-related dynamics of FD values of cerebral cortical ribbon and surface were the works of P. Podgórski et al. [5] and C.R. Madan and E.A. Kensinger [12].

In the study by P. Podgórski et al. [5] (N = 697, age 38–80 years), to elucidate the aging characteristics of the brain in men and women, both cortical fractal analysis and morphometric methods based on Euclidean geometry were employed. The authors described reductions in gray and white matter volumes, cortical thickness, and gyrification index with age, along with increases in cerebrospinal fluid volume and sulcal depth. This investigation involved the development of 3D maps of FD distribution across the cortical hemispheres. The findings revealed that cortical FD changed with age in both men and women, but these changes were observed in a smaller percentage of locations (2.0%) in men compared to women (2.7%). The authors established that both male and female brains began to age around 45 years, but in women, the cortex was affected earlier compared to men.

In the study by C.R. Madan and E.A. Kensinger [12] (N = 427, age 20–86 years), a 3D "dilation algorithm" (version of the "box-counting" method) was employed. The authors determined the FD values of cortical ribbon and its surface. It was established that both FD values significantly decreased with age: FD of cortical ribbon ($r = -0.732$) and the FD of 3D reconstruction of outer cortical surface ($r = -0.719$). Additionally, it was found that the average cortical thickness ($r = -0.603$) and gyrification index ($r = -0.494$) decreased with age.

In the study by K. Im et al. [6], a 3D variant of the "box-counting" method was also utilized. Using this method, the FD values of cortical surface were determined in 44 individuals. An interesting finding of this research was the correlation between the FD of the cerebral cortical surface and the intelligence quotient (IQ) and years of education; the results indicated a significant association between cortical surface FD and intelligence and education.

Another comprehensive study (S. Farahibozorg et al.) [13] (N = 209, age 20–80 years) was focused on age-related changes in the FD of the white matter of the brain. The authors also employed a 3D variant of the "box-counting" method and determined the FD values for white matter as a whole, its surface (boundary between cortex and white matter, which also constitutes the inner surface of the cortex), and the digital skeletons of the white matter. The authors found that the FD of white matter as a whole and its digital skeleton exhibited an inverse U-shaped relationship with age ($r^2 = 0.116$ and $r^2 = 0.202$, respectively); the correlation of the FD of the white matter surface with age was weaker ($r^2 = 0.040$).

In the study by L. Zhang et al. [14], an another 3D modification of the "box-counting" method was employed. The research, conducted on a small sample (N = 10, 8 young and 2 elderly individuals), revealed significant differences in the FD values for white matter as a whole, its surface, and its digital skeletons between young and old individuals.

2D variants of fractal analysis in studies of age-related changes in the brain have been relatively uncommon. In the work of E. Kalmanti and T. G. Maris [22], a 2D variant of the "box-counting" method was used to determine the FD values of cortex contours in parasagittal tomographic sections. The sample included 93 individuals aged from 3 months to 78 years. Unlike previous studies, this research encompassed the characterization of age-related changes in FD in children and adolescents: statistically significant correlations between FD and age were identified in different age groups (correlation coefficient r ranged from −0.08 to −0.497).

In addition to changes in cortical FD throughout the normal aging, alterations have been detected in pathological brain aging. For instance, in the studies conducted by R.D. King et al., where fractal analysis of the cortex of the cerebral hemispheres was performed using 2D [15] and 3D

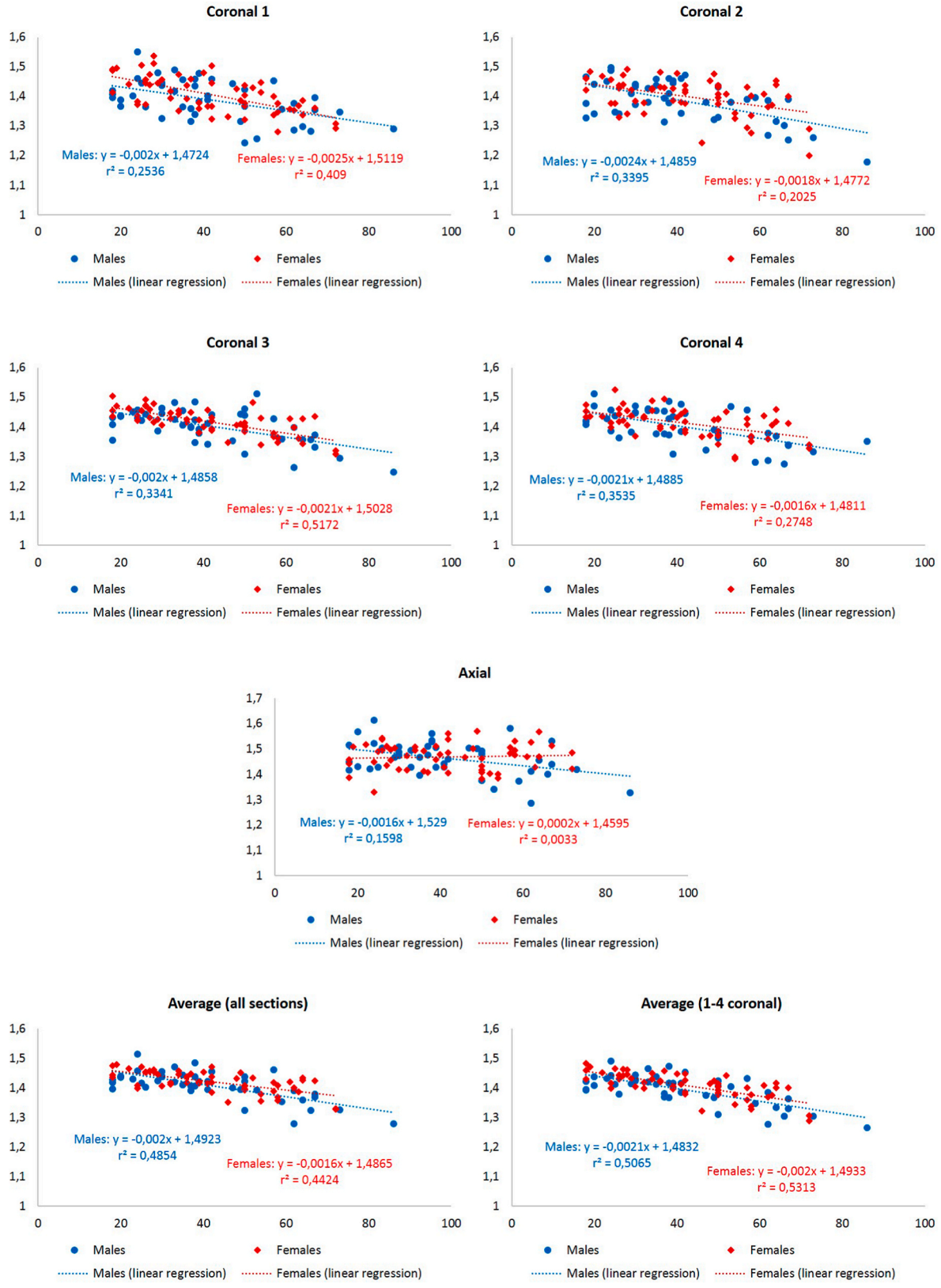

Fig. 10. Age dynamics of the FD values of cerebral hemispheres contour, computed using the "contour smoothing" method, employing 1–4 stages of fractal analysis: features in men and women.

Table 5
Correlation coefficients (r) characterizing relationships of FD values among tomographic sections of different localizations.

Tomographic section	1st coronal	2nd coronal	3rd coronal	4th coronal
2nd coronal	0.521***	–		
3rd coronal	0.496***	0.549***	–	
4th coronal	0.389***	0.446***	0.653***	–
Axial	0.294**	0.227*	0.260**	0.265**

Note: * – $p < 0.05$; ** – $p < 0.01$; *** – $p < 0.001$, Student T test.

[16] modifications of the "box-counting" method, statistically significant reductions in the FD values of cortical ribbon were observed in patients with Alzheimer's disease compared to healthy individuals.

In our previous studies conducted on the same sample as in the present work, we utilized a 2D variant of the "box-counting" method for fractal analysis of silhouette images [29] and skeletonized images [30]. In the investigation of silhouette images, the following correlation coefficients between FD values and age were identified: 1st coronal section ($r = -0.232$, $p < 0.05$), 2nd coronal section ($r = -0.511$, $p < 0.001$), 3rd coronal section ($r = -0.429$, $p < 0.001$), 4th coronal section ($r = -0.312$, $p < 0.01$), axial section ($r = -0.313$, $p < 0.01$), average FD value of all tomographic sections ($r = -0.512$, $p < 0.001$), and average FD value of 1–4 coronal sections ($r = -0.491$, $p < 0.001$) [29]. In the study of skeletonized images, the following correlation coefficients between FD values and age were identified: 1st coronal section ($r = -0.22$, $p < 0.05$), 2nd coronal section ($r = -0.45$, $p < 0.001$), 3rd coronal section ($r = -0.26$, $p < 0.01$), 4th coronal section ($r = -0.39$, $p < 0.001$), axial section ($r = 0.09$, $p > 0.05$), average FD value of all tomographic sections ($r = -0.40$, $p < 0.001$), and average FD value of 1–4 coronal sections ($r = -0.46$, $p < 0.001$) [30].

Thus, in this and previous works, we employed four variants of 2D MRI image fractal analysis: fractal analysis of silhouette [29] and skeletonized [30] images using the classical "box-counting" method, as well as fractal analysis of the linear contour of cerebral hemispheres using both the classical "box-counting" method and the "contour smoothing" method developed by us, described in this paper. Considering that all four fractal analysis variants were applied to the same sample, and its size was sufficient for obtaining statistically significant results ($N = 100$), it can be argued that the most informative 2D variant of fractal analysis employed in these studies for detecting age-related atrophic changes was the "contour smoothing method". Analysis of cerebral hemispheres' contour using the classical "box-counting" method was not sensitive to age-related changes, while silhouette and skeletonized image investigations using the same method exhibited moderate sensitivity to detecting age-related changes.

However, can our proposed 2D variant of fractal analysis be as sensitive to detecting age-related changes as 3D variants? Among the works of other authors that employed 3D fractal analysis variants in their studies, the strongest correlations between age and FD of cortical ribbon and its surface were found in the study by C.R. Madan and E.A. Kensinger [12] ($r = -0.732$ and $r = -0.719$, respectively). It is conceivable that the methodology utilized in this study has proven to be the most sensitive for detecting and characterizing atrophic changes. These correlation coefficient values between FD and age are close to those obtained in our study ($r = -0.709$ for the average FD value of four coronal sections). The proximity of the results may support the likelihood and reproducibility of the results obtained through fractal analysis methods used in both studies.

The main advantages of the fractal analysis method proposed in the present study are its simplicity and ease of implementation in clinical practice. This research approach does not require the construction of 3D models or image pre-processing. Fractal analysis can be applied to various types of images, including MRI images and other image formats (grayscale, color, including macrophotographs of anatomical sections); tomographic or anatomical sections of varying thickness can also be utilized. The primary requirement for the images under investigation is the ability for visual identification of the pial surface for contour selection by graphic editor software. Thus, even images obtained from MRI scanners with low magnetic induction values (which are commonly used in daily clinical practice in developing countries) can be used for fractal analysis, if they allow a clear defining the pial surface of the cortex. This surface is typically clearly identifiable even in low-quality MRI images, making its visual identification in most cases feasible. In comparison, the boundary between the cortex and white matter is less distinct, making it more challenging to accurately identify on low-quality images. Considering this, when using images of insufficient quality, preference should be given to investigating the pial surface of the cortex rather than the cortical ribbon or its boundary with white matter.

In our study, we utilized Adobe Photoshop CS5 software for "contour smoothing" method development; however, other graphic editors equipped with tools for contour selection, smoothing, and length measurement can also be employed for this analysis method. To expedite and automate analysis, a sequence of actions using Adobe Photoshop can be recorded, allowing subsequent processes to be automated after initial contour selection.

Another advantage of the 2D approach over 3D fractal analysis variants is the ability to investigate specific tomographic or anatomical sections for identifying local pathological changes.

Our study faced limitations in terms of the relatively small sample size (100) and the limited number of sections chosen for investigation (4 coronal and 1 axial). Potential constraints for the application of our developed fractal analysis method may include poor MRI image quality and the presence of artifacts (when defining the pial surface contour of the cerebral hemispheres is unclear), inability to use graphic editors or proficiency in operating such software. This fractal analysis method cannot be used to determine the FD of the entire cortical ribbon or the FD of solid objects, as it solely calculates the FD of the contour (surface) without accounting for cortical thickness or volume of solid object. Therefore, the contour smoothing method may prove useful for

Table 6
Correlation coefficients (r) characterizing relationships between FD values and morphometric parameters determined using Euclidean geometry methods.

Morphometric parameter		Tomographic section				
		1st coronal	2nd coronal	3rd coronal	4th coronal	Axial
P_A	Perimeter	0.060	−0.004	−0.169	−0.145	−0.252*
A_A	Area	0.227*	−0.002	−0.036	−0.075	−0.212*
P_A/A_A	Ratio of perimeter and area	−0.321***	0.002	−0.097	−0.003	0.047
SF_A	Shape Factor	0.381***	0.012	0.221*	0.167	0.069
P_B	Perimeter	0.337***	0.344***	0.250*	0.367***	0.257*
A_B	Area	0.460***	0.272**	0.238*	0.139	−0.164
P_B/A_B	Ratio of perimeter and area	−0.209*	0.071	0.008	0.203*	0.392***
SF_B	Shape Factor	−0.081	−0.227***	−0.116	−0.292**	−0.464***
P_B/P_A	Ratio of perimeter values (2D gyrification index)	0.388***	0.393***	0.383***	0.519***	0.454***
A_B/A_A	Ratio of area values	0.656***	0.660***	0.575***	0.527***	0.042

Note: * – $p < 0.05$; ** – $p < 0.01$; *** – $p < 0.001$, Student T test.

examining linear objects (such as contours and surfaces) and is particularly insightful when assessing the FD of irregular curves (e.g., cerebral cortex) without factoring in their thickness, especially in situations where such information is necessary.

5. Conclusion

The "contour smoothing" fractal analysis method introduced in this study can effectively examine cerebral hemispheres to detect and quantify age-related atrophic changes associated with normal or pathological aging. Furthermore, this fractal analysis method holds promise for clinical application in diagnosing neurodegenerative disorders, such as Alzheimer's disease.

Ethical statement

The study was conducted in accordance with the Declaration of Helsinki, and approved by the Commission on Ethics and Bioethics of Kharkiv National Medical University (minutes of the meeting of the Commission on Ethics and Bioethics of KhNMU No. 10 of Nov. 7, 2018) for studies involving humans. Written informed consent has been obtained from the participants of the study.

Funding

This research did not receive any specific grant from funding agencies in the public, commercial, or not-for-profit sectors.

CRediT authorship contribution statement

Nataliia Maryenko: Conceptualization, Data curation, Formal analysis, Investigation, Methodology, Software, Visualization, Writing – original draft. **Oleksandr Stepanenko:** Conceptualization, Methodology, Project administration, Supervision, Validation, Writing – review & editing.

Declaration of competing interest

The authors have no competing interests to declare.

Acknowledgments

The authors would like to express their sincere gratitude to the participants of this study, without whom this research would not have been possible.

Appendix A. Supplementary data

Supplementary data to this article can be found online at https://doi.org/10.1016/j.tria.2023.100263.

Abbreviations

A	area
FD	fractal dimension
MRI	magnetic resonance imaging
P	perimeter
R	smoothing radius
SF	shape factor
2D	two-dimensional
3D	three-dimensional

References

[1] Y. Ge, R.I. Grossman, J.S. Babb, M.L. Rabin, L.J. Mannon, D.L. Kolson, Age-related total gray matter and white matter changes in normal adult brain. Part I: volumetric MR imaging analysis, AJNR Am. J. Neuroradiol. 23 (8) (2002) 1327–1333.
[2] K.B. Walhovd, A.M. Fjell, I. Reinvang, A. Lundervold, A.M. Dale, D.E. Eilertsen, B. T. Quinn, D. Salat, N. Makris, B. Fischl, Effects of age on volumes of cortex, white matter and subcortical structures, Neurobiol. Aging 26 (9) (2005 Oct) 1261–1270, https://doi.org/10.1016/j.neurobiolaging.2005.05.020. ; discussion 1275-8.
[3] R. Riello, F. Sabattoli, A. Beltramello, M. Bonetti, G. Bono, A. Falini, G. Magnani, G. Minonzio, E. Piovan, G. Alaimo, M. Ettori, S. Galluzzi, E. Locatelli, M. Noiszewska, C. Testa, G.B. Frisoni, Brain volumes in healthy adults aged 40 years and over: a voxel-based morphometry study, Aging Clin. Exp. Res. 17 (4) (2005 Aug) 329–336, https://doi.org/10.1007/BF03324618.
[4] F. Zheng, Y. Liu, Z. Yuan, X. Gao, Y. He, X. Liu, D. Cui, R. Qi, T. Chen, J. Qiu, Age-related changes in cortical and subcortical structures of healthy adult brains: a surface-based morphometry study, J. Magn. Reson. Imag. 49 (1) (2019 Jan) 152–163, https://doi.org/10.1002/jmri.26037.
[5] P. Podgórski, J. Bladowska, M. Sasiadek, A. Zimny, Novel volumetric and surface-based magnetic resonance indices of the aging brain - does male and female brain age in the same way? Front. Neurol. 12 (2021 Jun 7), 645729 https://doi.org/10.3389/fneur.2021.645729.
[6] K. Im, J.M. Lee, U. Yoon, Y.W. Shin, S.B. Hong, I.Y. Kim, J.S. Kwon, S.I. Kim, Fractal dimension in human cortical surface: multiple regression analysis with cortical thickness, sulcal depth, and folding area, Hum. Brain Mapp. 27 (12) (2006 Dec) 994–1003, https://doi.org/10.1002/hbm.20238.
[7] H. Matsuda, MRI morphometry in Alzheimer's disease, Ageing Res. Rev. 30 (2016) 17–24, https://doi.org/10.1016/j.arr.2016.01.003.
[8] L. Pini, M. Pievani, M. Bocchetta, et al., Brain atrophy in Alzheimer's Disease and aging, Ageing Res. Rev. 30 (2016) 25–48, https://doi.org/10.1016/j.arr.2016.01.002.
[9] J.L. Whitwell, Alzheimer's disease neuroimaging, Curr. Opin. Neurol. 31 (4) (2018) 396–404, https://doi.org/10.1097/WCO.0000000000000570.
[10] B.B. Mandelbrot, Fractals – Form, Chance and Dimension, W.H. Freeman and Company, San Francisco, 1977.
[11] B.B. Mandelbrot, The Fractal Geometry of Nature, W.H. Freeman and Company, San Francisco, 1982.
[12] C.R. Madan, E.A. Kensinger, Cortical complexity as a measure of age-related brain atrophy, Neuroimage 134 (2016 Jul 1) 617–629, https://doi.org/10.1016/j.neuroimage.2016.04.029.
[13] S. Farahibozorg, S.M. Hashemi-Golpayegani, J. Ashburner, Age- and sex-related variations in the brain white matter fractal dimension throughout adulthood: an MRI study, Clin. Neuroradiol. 25 (1) (2015 Mar) 19–32, https://doi.org/10.1007/s00062-013-0273-3.
[14] L. Zhang, D. Dean, J.Z. Liu, V. Sahgal, X. Wang, G.H. Yue, Quantifying degeneration of white matter in normal aging using fractal dimension, Neurobiol. Aging 28 (10) (2007 Oct) 1543–1555, https://doi.org/10.1016/j.neurobiolaging.2006.06.020.
[15] R.D. King, A.T. George, T. Jeon, L.S. Hynan, T.S. Youn, D.N. Kennedy, B. Dickerson, The alzheimer's disease neuroimaging initiative. Characterization of atrophic changes in the cerebral cortex using fractal dimensional analysis, Brain Imag. Behav. 3 (2) (2009 Jun) 154–166, https://doi.org/10.1007/s11682-008-9057-9.
[16] R.D. King, B. Brown, M. Hwang, T. Jeon, A.T. George, Alzheimer's Disease Neuroimaging Initiative. Fractal dimension analysis of the cortical ribbon in mild Alzheimer's disease, Neuroimage 53 (2) (2010 Nov 1) 471–479, https://doi.org/10.1016/j.neuroimage.2010.06.050.
[17] F.J. Esteban, J. Sepulcre, J.R. de Miras, J. Navas, N.V. de Mendizábal, J. Goñi, et al., Fractal dimension analysis of grey matter in multiple sclerosis, J. Neurol. Sci. 282 (1–2) (2009 Jul 15) 67–71, https://doi.org/10.1016/j.jns.2008.12.023.
[18] F.J. Esteban, J. Sepulcre, N.V. de Mendizábal, et al., Fractal dimension and white matter changes in multiple sclerosis, Neuroimage 36 (3) (2007) 543–549, https://doi.org/10.1016/j.neuroimage.2007.03.057.
[19] E. Roura, G. Maclair, M. Andorrà, et al., Cortical fractal dimension predicts disability worsening in Multiple Sclerosis patients, Neuroimage Clin. 30 (2021), 102653, https://doi.org/10.1016/j.nicl.2021.102653.
[20] E.T. Ziukelis, E. Mak, M.E. Dounavi, L. Su, J. T O'Brien, Fractal dimension of the brain in neurodegenerative disease and dementia: a systematic review, Ageing Res. Rev. 79 (2022), 101651, https://doi.org/10.1016/j.arr.2022.101651.
[21] A. Di Ieva, F.J. Esteban, F. Grizzi, W. Klonowski, M. Martín-Landrove, Fractals in the neurosciences, Part II: clinical applications and future perspectives, Neuroscientist 21 (1) (2015 Feb) 30–43, https://doi.org/10.1177/1073858413513928.
[22] E. Kalmanti, T.G. Maris, Fractal dimension as an index of brain cortical changes throughout life, In Vivo 21 (4) (2007) 641–646.
[23] V.G. Kiselev, K.R. Hahn, D.P. Auer, Is the brain cortex a fractal? Neuroimage 20 (3) (2003 Nov) 1765–1774, https://doi.org/10.1016/s1053-8119(03)00380-x.
[24] B. Mandelbrot, How long is the coast of britain? Statistical self-similarity and fractional dimension, Science 156 (3775) (1967) 636–638, https://doi.org/10.1126/science.156.3775.636.
[25] I. Zaletel, D. Ristanović, B.D. Stefanović, N. Puškaš, Modified Richardson's method versus the box-counting method in neuroscience, J. Neurosci. Methods 242 (2015) 93–96, https://doi.org/10.1016/j.jneumeth.2015.01.013.
[26] N. Maryenko, O. Stepanenko, Fractal analysis as a method of morphometric study of linear anatomical objects: modified Caliper method, Rep. Morphology 27 (4) (2021) 28–34, https://doi.org/10.31393/morphology-journal-2021-27(4)-04.
[27] C.A. Schneider, W.S. Rasband, K.W. Eliceiri, NIH Image to ImageJ: 25 years of image analysis, Nat. Methods 9 (7) (2012) 671–675, https://doi.org/10.1038/nmeth.2089.

[28] E.E. Underwood, Quantitative Stereology, Addison-Wesley, London, 1970.
[29] N. Maryenko, O. Stepanenko, Fractal dimension of silhouette magnetic resonance brain images as a measure of age-associated changes in cerebral hemispheres, Duzce Med. J. 25 (1) (2023) 27–37, https://doi.org/10.18678/dtfd.1180625.
[30] N.I. Maryenko, O.Y. Stepanenko, Fractal dimension of skeletonized MR images as a measure of cerebral hemispheres spatial complexity, Rep. Morphology 28 (2) (2022) 40–47, https://doi.org/10.31393/morphology-journal-2022-28(2)-06.